Journal of Computational Physics 228 (2009) 7805–7820

Contents lists available at ScienceDirect

Journal of Computational Physics

journal homepage: www.elsevier.com/locate/jcp

An operator splitting method for the Degasperis–Procesi equation

B.-F. Feng [a,*], Y. Liu [b,*]

[a] Department of Mathematics, The University of Texas-Pan American, Edinburg 78541, United States
[b] Department of Mathematics, The University of Texas-Arlington, United States

ARTICLE INFO

Article history:
Received 1 January 2009
Received in revised form 22 July 2009
Accepted 27 July 2009
Available online 6 August 2009

ABSTRACT

An operator splitting method is proposed for the Degasperis–Procesi (DP) equation, by which the DP equation is decomposed into the Burgers equation and the Benjamin–Bona–Mahony (BBM) equation. Then, a second-order TVD scheme is applied for the Burgers equation, and a linearized implicit finite difference method is used for the BBM equation. Furthermore, the Strang splitting approach is used to construct the solution in one time step. The numerical solutions of the DP equation agree with exact solutions, e.g. the multipeakon solutions very well. The proposed method also captures the formation and propagation of shockpeakon solutions, and reveals wave breaking phenomena with good accuracy.

Published by Elsevier Inc.

1. Introduction

In this paper, we present an operator splitting method for the numerical solutions of the Degasperis–Procesi equation [19]

$$u_t + 3\kappa^3 u_x - u_{xxt} + 4uu_x = 3u_x u_{xx} + uu_{xxx}. \tag{1}$$

Degasperis and Procesi [19] studied a family of third order dispersive nonlinear equations

$$u_t - \alpha^2 u_{xxt} + \gamma u_{xxx} + c_0 u_x = (c_1 u^2 + c_2 u_x^2 + c_3 u u_{xx})_x, \tag{2}$$

with six real constants $c_0, c_1, c_2, c_3, \gamma, \alpha \in \mathbb{R}$. They found that there are only three equations were asymptotically integrable, i.e. the Korteweg-de Vries (KdV) equation ($\alpha = c_2 = c_3 = 0$), the Camassa–Holm (CH) equation ($c_1 = -\frac{3c_3}{2\alpha^2}, c_2 = \frac{c_3}{2}$), and one new equation ($c_1 = -\frac{2c_3}{\alpha^2}, c_2 = c_3$), which is named the Degasperis–Procesi (DP) equation later on.

The Camassa–Holm equation

$$u_t + 2\kappa^2 u_x - u_{xxt} + 3uu_x = 2u_x u_{xx} + uu_{xxx}, \tag{3}$$

was first derived by Fokas and Fuchssteiner [24] as a bi-Hamiltonian system and then has attracted considerable attention since it was derived as a model equation for shallow water waves in 1993 [4]. The Camassa–Holm equation has been shown to be completely integrable [5]. Explicit form of multipeakon solutions for the Camassa–Holm equation was found by Beals et al. when $k \neq 0$ [2]. An approach based on the inverse scattering transform method (IST) provides an explicit form of the inverse mapping in terms of Wronskian [15].

The Degasperis–Procesi equation only differs from the Camassa–Holm equation by coefficients. Degasperis et al. proved the integrability of the DP equation by constructing a Lax pair and a bi-Hamiltonian structure [18]. These two equations share some common properties. They both can be viewed as the models of shallow water waves [4,5,31,16]. When $\kappa \neq 0$, the Camassa–Holm equation is related to the AKNS shallow water wave equation by a hodograph transformation [41],

* Corresponding author.
E-mail address: feng@utpa.edu (B.-F. Feng).

0021-9991/$ - see front matter Published by Elsevier Inc.
doi:10.1016/j.jcp.2009.07.022

and the Degasperis–Procesi equation is related to the Hirota-Satsuma shallow water wave equation by a similar hodograph transformation [37]. By use of the above findings, Matsuno obtained the multisoliton solutions of the DP equation when $\kappa \neq 0$ [37,38]. When $\kappa = 0$, both the CH and the DP equations have multipeakon solutions, the explicit form of multipeakon solution of the DP equation was found by Lundmark and Szmigielski by solving an inverse scattering problem of a discrete cubic string [34,35]. Furthermore, the peakon solutions for both the CH equation and the DP equation are orbitally stable [17,32].

On the other hand, although the DP equation has an apparent similarity to the CH equation, there are major structural differences between these two equations such as the Lax pair, wave breaking phenomena and the solutions. The isospectral problem in the Lax pair for the DP equation is the third-order equation [18], while the isospectral problem for the CH equation is the second order equation [4]. It is worth noting that Lundmark [36] showed that, when $\kappa = 0$, the DP equation has not only one peakon solution, $u(x,t) = ce^{-|x-ct|}$ but also a shock peakon solution of the form

$$u(x,t) = ce^{-|x-ct|} + \operatorname{sgn}(x-ct)\frac{s}{1+ts}e^{-|x-ct|}, \tag{4}$$

where $c, s (s > 0)$ are constants. Moreover, it is recently shown by Escher et al. [21] that the DP equation possesses a periodic shock wave solution given by

$$u(x,t) = \begin{cases} \left(\frac{\cosh\left(\frac{1}{2}\right)}{\sinh\left(\frac{1}{2}\right)}t + c\right)^{-1} \frac{\sinh\left(x-[x]-\frac{1}{2}\right)}{\sinh\left(\frac{1}{2}\right)}, & x \in \mathbb{R}\setminus\mathbb{Z},\ c > 0, \\ 0, & x \in \mathbb{Z}. \end{cases}$$

Lundmark further extended the multipeakon solution of the DP equation to multi-shockpeakon solution [36]

$$u(x,t) = \sum_{i=1}^{n} m_i(t)e^{-|x-x_i(t)|} + \sum_{i=1}^{n} s_i(t)\operatorname{sgn}(x-x_i)e^{-|x-x_i(t)|}, \tag{5}$$

where $m_i(t), x_i(t)$ and $s_i(t)$ stand for the momentum, position and strength of the ith shockpeakon. It is shown that (5) is a weak solution of the DP equation if and only if $m_i(t), x_i(t)$ and $s_i(t), i = 1, \ldots, n$ satisfy a system of ODEs ((2.4) and (2.5) in [36]). However, the integrability and the explicit form of above solution are still unclear even for $n = 2$ case. The only explicit form available is one shockpeakon solution mentioned above in (4).

Note that these peakons and shockpeakons are not the strong solutions in the Sobolev space $H^s, s \geqslant \frac{3}{2}$, but the global weak solutions in H^1 [20]. Existence of these discontinuous (shock waves, [36]) solutions of the DP equation shows that the DP equation would behave radically different from the Camassa–Holm equation, but similar to the inviscid Burgers equation, which implies that a well-posedness theory should depend on some functional spaces which contain discontinuous functions. Indeed, this observation was confirmed by Coclite and Karlsen [11–13]. In [11–13], they proved the global existence and uniqueness of $L^1 \cap BV$ entropy weak solutions satisfying an infinite family of Kružkov-type entropy inequalities. and also proved existence of bounded weak solutions by an Oleĭnik-type estimate for L^∞ solutions to the DP equation with $\kappa = 0$.

For the purpose of numerical tests, the explicit form of two-peakon solution $u(x,t) = \sum_{i=1}^{2} m_i(t)e^{-|x-x_i(t)|}$ is listed here.

$$x_1(t) = \log\frac{(\lambda_1-\lambda_2)^2 b_1 b_2}{(\lambda_1+\lambda_2)(\lambda_1 b_1 + \lambda_2 b_2)}, \quad x_2(t) = \log(b_1+b_2), \tag{6}$$

$$m_1(t) = \frac{(\lambda_1 b_1 + \lambda_2 b_2)^2}{\lambda_1\lambda_2\left(\lambda_1 b_1^2 + \lambda_2 b_2^2 + \frac{4\lambda_1\lambda_2}{\lambda_1+\lambda_2} b_1 b_2\right)}, \quad m_2(t) = \frac{(b_1+b_2)^2}{\lambda_1 b_1^2 + \lambda_2 b_2^2 + \frac{4\lambda_1\lambda_2}{\lambda_1+\lambda_2} b_1 b_2}, \tag{7}$$

with $b_k(t) = b_k(0)e^{t/\lambda_k}$. Here λ_1, λ_2 are nonzero distinct constants, and $b_1(0)$ and $b_2(0)$ are two positive constants.

In the last decade, a lot of numerical schemes have been proposed for the Camassa–Holm equation. These include pseudo-spectral method [29], finite difference schemes [27,10], a finite volume method [1], a finite element method [43], multi-symplectic methods [14], a particle method based on the multipeakon solutions of the Camassa–Holm equation [6–8,28], an energy-conserving Galerkin scheme [39], and a self-adaptive mesh method based on an integrable semi-discretization of the Camassa–Holm equation [40,23]. On the contrary, the numerical methods available for the Degasperis–Procesi equation are only a few. Coclite et al. proposed several operator splitting schemes for the DP equation and proved convergence of those finite difference schemes to entropy weak solutions [10]. On the other hand, Hoel investigated entropy weak solutions of the DP equation numerically by a particle method based on the multi-shockpeakon solutions [26]. It is necessary to construct more effective numerical methods for the Degasperis–Procesi equation. The purpose of the present paper is to provide an operator splitting method for the numerical simulations of discontinuous solutions of the DP equation.

The remainder of the present paper is organized as follows. in Section 2, we present the operator splitting strategy, by which the Degasperis–Procesi equation is decomposed into the Burgers equation and the Benjamin–Bona–Mahony (BBM) equation. Then, extensive numerical experiments are performed in Section 3. These include peakon propagation and interactions, peakon–antipeakon interactions, shockpeakon–shockpeakon interactions, as well as initial value problems for some nonexact initial conditions. A good agreement is obtained in comparing exact and numerical solutions. In addition, the theoretical results of wave breaking phenomena are verified and explored numerically. Concluding remarks and comments are given in Section 4.

2. Numerical method based on operator splitting

2.1. Strategy of operator splitting method

First, we introduce some notations for the use of numerical scheme of the DP equation. Suppose the computational domain $[0, L]$ is divided into $N+1$ equispaced grid points with spacing $\Delta x = L/N$. u_l^n denotes the approximate solution for the exact solution $u(l\Delta x, n\Delta t)$.

It is known that the DP equation can be written as a hyperbolic-elliptic system

$$u_t + f_x(u) + P_x = 0, \quad P - P_{xx} = 3\kappa^3 u + 3f(u), \tag{8}$$

where $f(u) = \frac{1}{2}u^2$. Eq. (8) is the starting point for defining weak solutions and proving well-posedness of the DP equation. It is also an appropriate form for us to design a numerical scheme.

The numerical schemes in [9] are constructed based on Eq. (8). The operator splitting strategy we used is as follows. Let $H_t u_0$ and $D_t u_0$ denote the solution of the Cauchy problems

$$u_t + f_x(u) = 0, \quad u(x,0) = u_0(x), \tag{9}$$

$$u_t + P_x = 0, \quad u(x,0) = u_0(x), \tag{10}$$

respectively.

Note that Eq. (9) is nothing but the Burgers equation, and Eq. (10) is actually equivalent to the Benjamin–Bona–Mahony (BBM) equation [3]

$$u_t - u_{xxt} + \left(3\kappa^3 u + \frac{3}{2}u^2\right)_x = 0, \quad u(x,0) = u_0(x). \tag{11}$$

by use of Eq. (8).

In summary, the DP equation is decomposed into the Burgers equation and the Benjamin–Bona–Mahony (BBM) equation. To some extent, this decomposition reflects the mechanisms of shock formation in the DP equation. The construction of the numerical scheme will also be based on this decomposition. By applying a second order TVD scheme for the Burgers equation, and a linearized second order scheme for the BBM equation, the Strang splitting method [42] is applied and combine the two schemes to achieve a second order accuracy for the DP equation. The idea is to solve Eqs. (9) and (10) sequentially, and the numerical solution of the DP equation is constructed as

$$u_l^{n+1} = H_{\frac{1}{2}\Delta t} D_{\Delta t} H_{\frac{1}{2}\Delta t} u_l^n. \tag{12}$$

2.2. Second order TVD scheme for the hyperbolic equation

The formation of shock waves lies in the nature of the Burgers equation, which is a prototype equation to test all kinds of shock-capturing methods. Over the past 30 years, a great deal of progress has been made in this direction, and varieties of such methods are available. Examples include higher order Total Variation Diminishing (TVD) schemes first proposed by Harten [25] and Weighted Essentially Non-Oscillatory schemes (WENO).

It turns out that the TVD property of a scheme can be used as a nonlinear stability condition and together with consistency it guarantees the convergence of the numerical scheme [30].

Accordingly, a second order TVD scheme for the Burgers equation is proposed here. First we define

$$\bar{u}_l = \frac{f(u_l) - f(u_{l-1})}{u_l - u_{l-1}} = \frac{1}{2}(u_l + u_{l-1}), \tag{13}$$

and

$$r_{l-1/2} = \frac{\Delta u_{l-1/2}}{\Delta u_{l-1/2}},$$

where the index I is used to represent the interface on the *upwind* side of $x_{l-1/2}$:

$$I = \begin{cases} l-1 & \text{if } \bar{u}_l > 0 \\ l+1 & \text{if } \bar{u}_l < 0 \end{cases}$$

Furthermore, by letting $\lambda_l = \frac{\Delta t}{\Delta x}\bar{u}_l$, a second order TVD scheme takes the form

$$u_l^{n+1} = u_l^n - \frac{\Delta t}{\Delta x}(f(u_l^n) - f(u_{l-1}^n)) - \frac{1}{2}\lambda_l(1-\lambda_l)(\phi(r_{l+1/2})(u_{l+1}^n - u_l^n) - \phi(r_{l-1/2})(u_l^n - u_{l-1}^n)), \tag{14}$$

if $\bar{u}_l > 0$ (upwind), or

$$u_l^{n+1} = u_l^n - \frac{\Delta t}{\Delta x}(f(u_{l+1}^n) - f(u_l^n)) - \frac{1}{2}\lambda_l(1+\lambda_l)(\phi(r_{l+1/2})(u_{l+1}^n - u_l^n) - \phi(r_{l-1/2})(u_l^n - u_{l-1}^n)) \tag{15}$$

if $\bar{u}_l < 0$ (downwind).

Here $\phi(r_{l+1/2})$ are called flux-limiter functions, several popular choices which guarantees the TVD property are

$$\begin{aligned}&\text{minmod}: \quad \phi(r) = \text{minmod}(1, r),\\ &\text{superbee}: \quad \phi(r) = \max(0, \min(1, 2r), \min(2, r)),\\ &\text{MC}: \quad \phi(r) = \max(0, \min((1+r)/2, 2, 2r)),\\ &\text{vanLeer}: \quad \phi(r) = \tfrac{r+|r|}{1+|r|}.\end{aligned} \tag{16}$$

It is observed that minmod is the most diffusive limiter, it corresponds to the lower boundary of the TVD region, while superbee is the least diffusive limiter, it corresponds to the upper boundary of the TVD region. All of these produce second order scheme when the solution is smooth, and reduces to first order at discontinuities.

2.3. Linearized implicit finite difference method for the elliptic equation

We apply a linearized implicit finite difference method as proposed for the KdV equation by one of the authors [22] to the BBM equation (10). Through the Crank–Nicolson scheme, the BBM equation is discretized as

$$\left(1 - \frac{\delta_x^2}{\Delta x^2}\right)\frac{u_l^{n+1} - u_l^n}{\Delta t} + \frac{3}{2}\frac{H_x}{2\Delta x}(\kappa^3(u_l^n + u_l^{n+1}) + f_l^n + f_l^{n+1}) = 0, \tag{17}$$

where

$$\delta_x^2 u_l^n = u_{l+1}^n - 2u_l^n + u_{l-1}^n, \quad H_x u_l^n = u_{l+1}^n - u_{l-1}^n.$$

The nonlinear part in (17) can be approximated as

$$f_l^{n+1} + f_l^n = 2f_l^n + \left(\frac{\partial f}{\partial u}\right)_l^n \Delta u_l^{n+1} + O(\Delta t^2) = u_l^{n+1}u_l^n + O(\Delta t^2). \tag{18}$$

Substituting (18) into (17) yields the following tridiagonal system.

$$(-s - 0.75p(\kappa^3 + u_{l-1}^n))u_{l-1}^{n+1} + (1+2s)u_l^{n+1} + (-s + 0.75(\kappa^3 + u_{l+1}^n))u_{l+1}^{n+1} = d_l^n. \tag{19}$$

Here

$$p = \frac{\Delta t}{\Delta x}, \quad s = \frac{1}{(\Delta x)^2},$$

and

$$d_l^n = (1+2s)u_l^n - s(u_{l+1}^n + u_{l-1}^n) - 0.75p\kappa^3(u_{l+1}^n - u_{l-1}^n).$$

It is noted that we have to compute the coefficient matrix and d_l^n, then solve the tridiagonal system at each time step.

Similar to the analysis in [22], it can be easily shown that the order of linearized implicit method is of $O((\Delta x)^2, (\Delta t)^2)$. The method is unconditionally stable upon linear stability analysis. The proof is omitted here.

Since the proposed TVD scheme for the Burgers equation and the linearized implicit method for the BBM equation are both of the second order for smooth solutions, and the Strang splitting method also gives a truncation error of $O((\Delta t)^2)$. Hence, the operator splitting method for the DP equation is a second order method for smooth solutions. This is confirmed by numerical examples shown in the following subsequent section.

3. Numerical experiments

This section is to present extensive test problems of the DP equation for application of the splitting method. These include (1) single soliton propagation including the single smooth soliton when $\kappa \neq 0$ and the single peakon when $\kappa = 0$; (2) Binary peakon–peakon, peakon–antipeakon, shockpeakon–shockpeakon interactions and a triple peakon–antipeakon-shockpeakon interaction; (3) Initial value problems for several types of nonexact initial conditions. Periodic boundary condition is employed, which is conventional for the simulation of wave phenomena. All simulations use a fixed ratio $\Delta t = \frac{1}{2}\Delta x \max|U_j^n|$ to assure the CFL condition.

3.1. Single soliton solutions

We first check the accuracy and the order of the splitting scheme by a smooth solution.

Example 3.1. *Single smooth soliton*: when $\kappa \neq 0$ the DP Eq. (1) admits smooth N-soliton solutions in the parametric form [37], in which a smooth one-soliton solution is of the form

$$u(y,t) = \frac{2\kappa^3(a_1^2-1)(4a_1^2-1}{a_1(\cosh\xi_1 + 2a_1 - a_1^{-1})} \tag{20}$$

$$x(y,t) = \frac{y}{\kappa} + \ln\left(\frac{\alpha_1 + 1 + (\alpha_1 - 1)e^{\xi_1}}{\alpha_1 - 1 + (\alpha_1 + 1)e^{\xi_1}}\right). \tag{21}$$

Here

$$\xi_1 = k_1\left(y - \frac{3\kappa^4}{1-\kappa^2k_1^2}t - y_0\right)$$

$$a_1 = \frac{1}{2}\sqrt{\frac{4-\kappa^2k_1^2}{1-\kappa^2k_1^2}}$$

$$\alpha_1 = \sqrt{\frac{(2a_1-1)(a_1+1)}{(2a_1+1)(a_1-1)}}.$$

The simulations are run in a domain $[-20,20]$ with parameters $\kappa = 0.511, \kappa k_1 = 0.8, y_0 = 0.0$ with 2^M grid points. Fig. 1 shows the numerical and the exact solution at $t = 10.0$ for $\Delta x = \Delta t = 0.3125$. The initial date is the dashed line. The L_∞ errors are calculated and are shown in Table 1. Here $L_\infty = \max|\tilde{u}_l - u_l|$, where $\tilde{u}_l$ and u_l are the numerical and the exact solutions, respectively. It is obvious that the proposed scheme is of second order for smooth solutions.

Example 3.2. *Single peakon solution:*

$$u(x,t) = ce^{-|x-ct|} \tag{22}$$

is a solution for the DP equation when $\kappa = 0$. The profile $u_0(x) = u(x,0)$ yields the initial condition. For our numerical simulations, we choose $c = 1$ and the computation domain to be $[-10,10]$.

For $N = 256$, Table 2 compares the errors in the L_∞-norm and two of the conservative quantities $I_1 = \int u(x)dx$ and $I_2 = \int u^3(x)dx$ for different flux limiter functions at $t = 4.0$. Here $E_1 = (\bar{I}_1 - I_1)/I_1$ and $E_2 = (\bar{I}_2 - I_2)/I_2$ indicate the relative errors in I_1 and I_2. $\bar{I}_i$ and $I_i (i = 1,2)$ stand for the numerical and exact values for the conserved quantities. Simpson's rule was employed for the numerical quadrature of the integrals.

From Table 2, we can conclude that superbee limiter function gives a relatively better result. We next consider the rate of convergence of the scheme for the single peakon problem. Table 3 displays the relative errors in I_1, I_3, L_∞-norm and an order estimate at $t = 4.0$. The superbee limiter function is used.

3.2. Interactions for peakons and shockpeakons

Example 3.3. *Peakon–peakon interaction:* it is shown in [36] that the DP equation has a two-peakon solution in the form of (6) and (7) when $\kappa = 0$. In the test problem, the parameters are chosen to have two peakons of amplitudes $A_1 = 2.0$ and $A_2 = 1.0$ initially located at $x_1 = -13.792$ and $x_2 = -4.0$, respectively. Then the interaction of these two peakons are solved numerically on a domain $[-20,20]$. We use two different grid points $N = 512, 1024$ and set the time step to assure the CFL

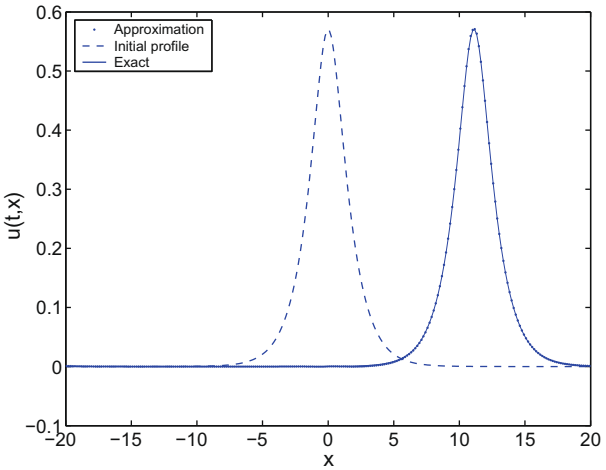

Fig. 1. Numerical solution of one smooth soliton solution.

Table 1
Convergence rate for a smooth soliton solution.

Δx	L_∞	Rate of convergence
40/64	9.125×10^{-2}	
40/128	2.778×10^{-2}	3.32
40/256	6.894×10^{-3}	4.03
40/512	1.740×10^{-3}	3.96

Table 2
Comparison of errors for different flux limiter functions.

Flux-limiter	L_∞	E_1	E_2
minmod	9.48×10^{-2}	-5.27×10^{-4}	-5.40×10^{-3}
vanLeer	7.03×10^{-2}	-4.84×10^{-4}	-3.02×10^{-3}
MC	5.97×10^{-2}	-4.80×10^{-4}	-2.43×10^{-3}
superbee	3.92×10^{-2}	-4.03×10^{-4}	-8.68×10^{-5}

Table 3
Convergence rate for one single peakon solution with $c = 1.0$.

Δx	E_1	E_2	L_∞	Order
20/128	-8.78×10^{-4}	-2.67×10^{-3}	1.1223×10^{-1}	
20/256	-4.03×10^{-4}	-8.68×10^{-5}	6.8893×10^{-2}	1.6291
20/512	-2.01×10^{-4}	3.13×10^{-4}	4.2700×10^{-2}	1.6134
20/1024	-1.18×10^{-4}	2.12×10^{-4}	3.6415×10^{-2}	1.1726
20/2048	-6.77×10^{-5}	8.36×10^{-5}	2.4607×10^{-2}	1.4798

condition. Only the superbee limiter function is used. Fig. 2 gives a 3D plot for the whole collision process, and Fig. 3 displays the snapshots at different times, together with the exact solution. Table 4 lists the relative errors in two conserved quantities E_1, E_2, and L_∞-norm at different stages of the interaction. The rate of the convergence is estimated for two different mesh sizes. Both the graph and the table indicate a good accuracy.

Example 3.4. *Peakon–antipeakon interaction:* the binary peakon–antipeakon interaction is theoretically studied by Lundmark [36]. We confirm his theoretical results for both the symmetric $(m_1 + m_2 = 0)$ and nonsymmetric $(m_1 + m_2 \neq 0)$ numerically. For the symmetric case, the parameters are chosen so that the peakon $(m_1 = 1.0)$ and antipeakon $(m_2 = -1.0)$ are located at $x_1 = -5.0$ and $x_2 = 5.0$ initially. Before the collision, the solution follows two-peakon solution (6) and (7). A stationary shockpeakon is formed at $t \approx 5.0$ with strength $s \approx 1.0$, and its evolution follows one shockpeakon solution (4). The numerical solutions verifies the theoretical prediction by Lundmark with good accuracy. Fig. 4 shows the

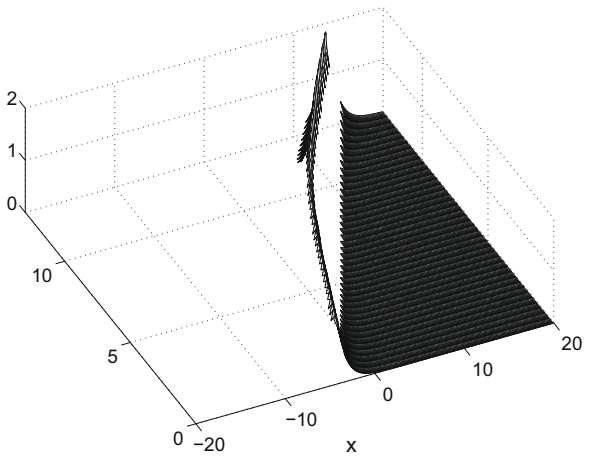

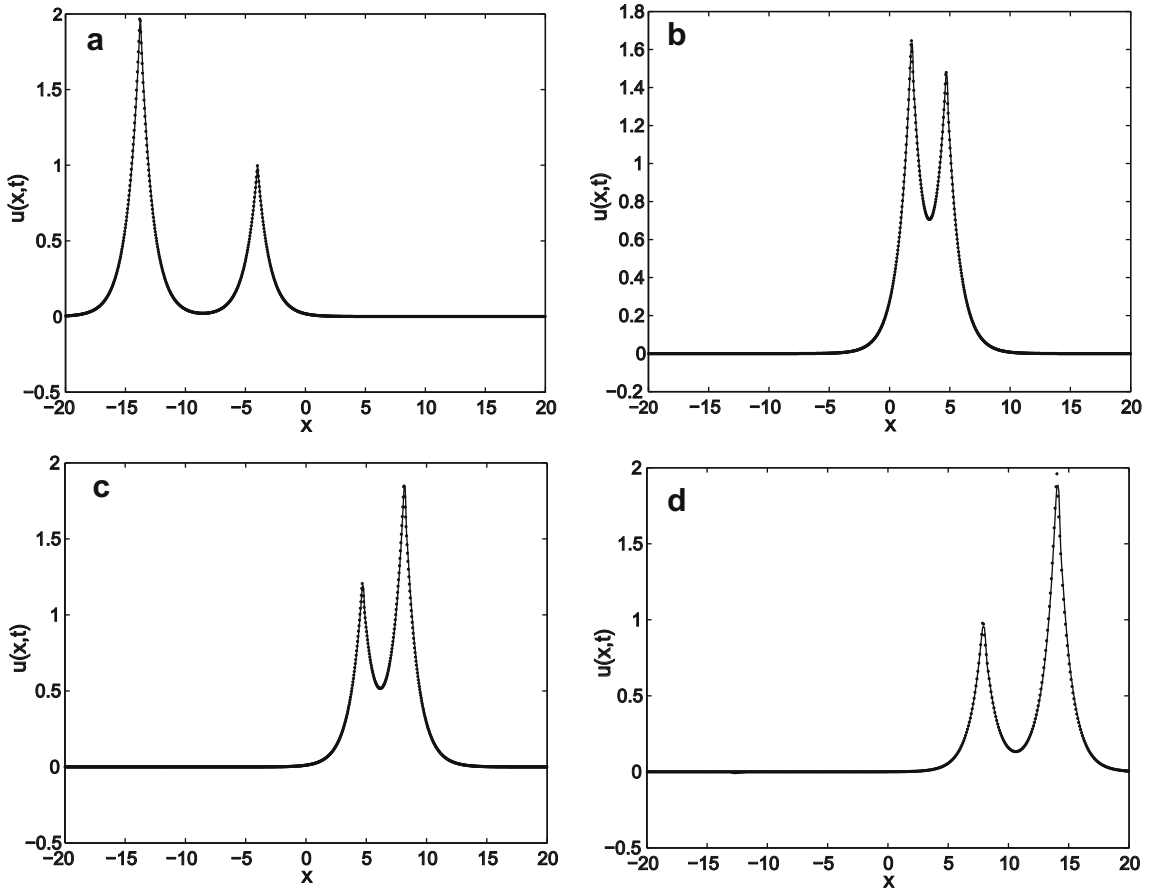

Fig. 3. Snapshots for the interaction of two peakon solutions (a) $t = 0.0$; (b) $t = 8.0$; (c) $t = 10.0$; (d) $t = 13.0$.

Table 4
Errors for two peakon interaction.

Time	Δx	E_1	E_2	L_∞	Order
$t = 2.0$	40/512	-5.06×10^{-4}	3.25×10^{-3}	9.5444×10^{-2}	
	40/1024	-6.29×10^{-4}	2.95×10^{-3}	3.9710×10^{-2}	2.4035
$t = 4.0$	40/512	-2.46×10^{-4}	6.27×10^{-3}	8.1185×10^{-2}	
	40/1024	-6.39×10^{-4}	6.28×10^{-3}	4.8175×10^{-2}	1.6852
$t = 6.0$	40/512	-4.30×10^{-4}	4.77×10^{-3}	6.1916×10^{-2}	
	40/1024	-6.61×10^{-4}	9.28×10^{-3}	4.2976×10^{-2}	1.4407
$t = 8.0$	40/512	-3.49×10^{-4}	5.76×10^{-3}	5.0201×10^{-2}	
	40/1024	-6.65×10^{-4}	1.18×10^{-2}	2.9882×10^{-2}	1.6802
$t = 10.0$	40/512	-3.22×10^{-4}	6.48×10^{-3}	6.2800×10^{-2}	
	40/1024	-6.63×10^{-4}	1.45×10^{-2}	4.8910×10^{-2}	1.2840

collision process before and after the collision. As mentioned in [36], I_3 is not a conserved quantity anymore. So in Table 5 we list the errors in I_1 and L_∞ at different times. It is worth noting that a convergence rate of about 1.0 is achieved once the shockpeakon is formed. This fact shows that the proposed method is especially effective for the simulations of discontinuous solutions.

For the nonsymmetric peakon–antipeakon interaction, the parameters are chosen as follows: $\lambda_1 = 0.5, \lambda_2 = -1.0, b_1(0) = 0.0015, b_2(0) = 148.4177$. Thus, initially, a peakon of amplitude 2.0 and an antipeakon of amplitude 1.0 are located at $x_1 = -5.0$ and $x_2 = 5.0$, respectively. Based on the results by Lundmark [36], two-peakon solution holds until $t < t_c = 3.3626$. At $t = t_c$, a moving shockpeakon is formed at $x = 1.8526$. One can calculate the momentum and the shock strength: $\tilde{m} = \lambda_1^{-1} + \lambda_2^{-1} = 1.0$, $\tilde{s} = \sqrt{-\lambda_1^{-1}\lambda_2^{-1}} = 1.4142$. The shockpeakon moves with a velocity of $\tilde{m} = 1.0$.

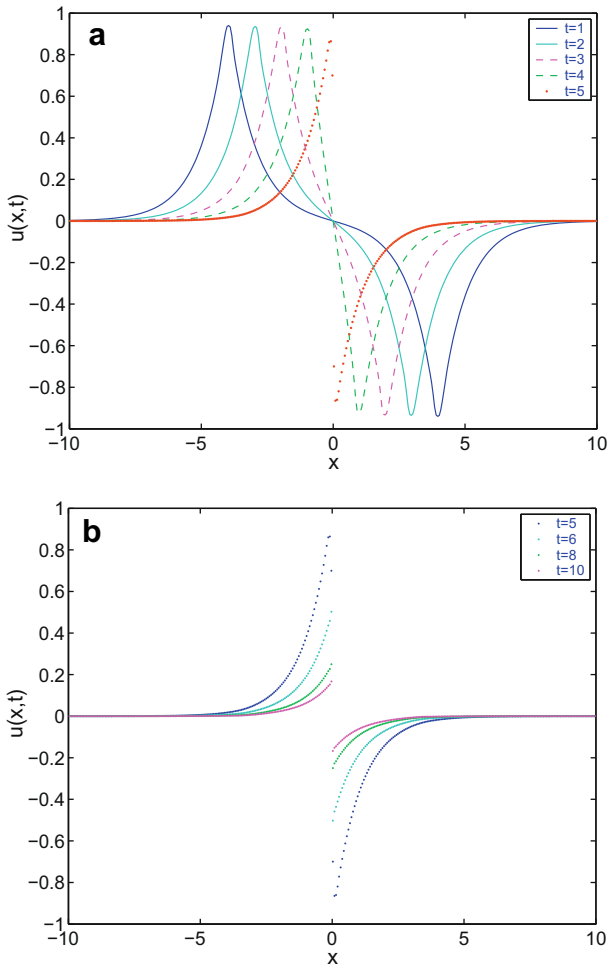

Fig. 4. Peakon–antipeakon interaction in the symmetric case: (a) before the collision; (b) after the collision.

The above theoretical predictions are confirmed by our scheme with good accuracy. Fig. 5 shows the snapshots of the numerical solutions before and after the collision. Table 6 displays the errors in L_∞ and E_1 for a fixed grid points $N = 1024$ in a computation domain $[-15, 15]$.

Example 3.5. *Shockpeakon–shockpeakon interaction:* as mentioned in [36], the shockpeakon dynamics still remains an open problem. Even for the case of $n = 2$, it is unclear whether the ODE system is integrable or not. There are difficulties in simulating the ODE system because the system behaves badly. However, the shockpeakon collisions can be studied through simulating the DP equation directly. To this end, we show an example whose initial condition is set to be

$$u(x,0) = \sum_{i=1}^{2} m_i(0) e^{-|x-x_{i0}|} + \sum_{i=1}^{2} s_i(0)\,\mathrm{sgn}(x - x_{i0}) e^{-|x-x_{i0}|}, \tag{23}$$

with $m_1(0) = 2.0, s_1(0) = 1.0, m_2(0) = 1.0, s_2(0) = -0.5, x_1(0) = -5.0$ and $x_2(0) = 5.0$. The numerical solutions is shown in Fig. 6 at different times, which clearly show that two shockpeakons merge into one shockpeakon at $t \approx 3.5$, then the resulting shockpeakon gains a momentum of $m = m_1 + m_2 = 1.0$ and moves to the right with velocity 1.0, following the solution (4).

Example 3.6. *A triple collision:* a triple collision among two symmetric peakon–antipeakons and one stationary shock peakon were studied theoretically by Lundmark in [36] and numerically by Coclite et al. in [9]. The initial condition for this case is

$$u(x,0) = e^{-|x+5|} + \mathrm{sgn}(x) e^{-|x|} - e^{-|x-5|}. \tag{24}$$

The exact solution will be a triple collision among a peakon, an antipeakon and a shockpeakon at $t = t_c \approx 5.32$ and $x = 0$. For $t > t_c$ the solution will merge into one single shock peakon.

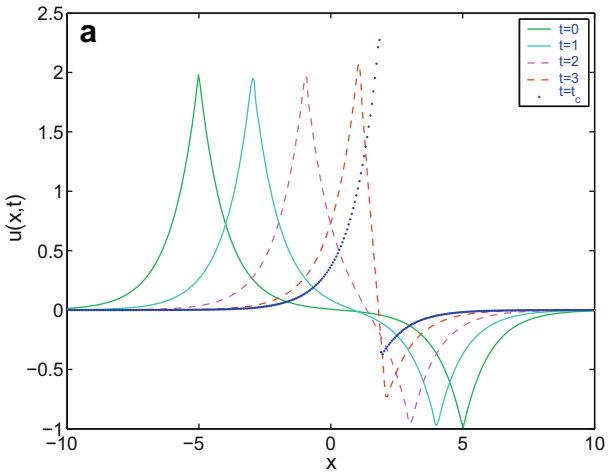

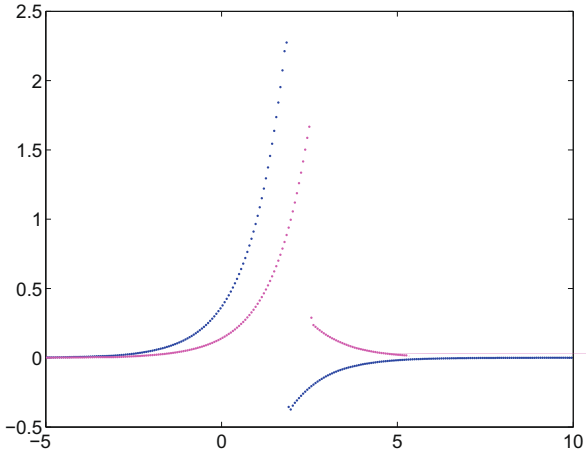

Table 5
Errors for peakon–antipeakon interaction in the symmetric case.

Time	Δx	I_1	L_∞	Order
$t = 2.0$	30/256	-1.51×10^{-5}	9.9171×10^{-2}	
	30/512	-1.63×10^{-4}	5.4572×10^{-2}	1.8173
	30/1024	3.59×10^{-5}	3.6461×10^{-2}	1.4967
$t = 4.0$	30/256	-4.37×10^{-5}	1.2477×10^{-1}	
	30/512	-4.64×10^{-4}	5.4145×10^{-2}	2.3043
	30/1024	-2.89×10^{-6}	3.9268×10^{-2}	1.3788
$t = 6.0$	30/256	-7.07×10^{-3}	3.5888×10^{-2}	
	30/512	-2.96×10^{-3}	1.6728×10^{-2}	2.1453
	30/1024	-1.34×10^{-3}	6.4997×10^{-3}	2.5737
$t = 8.0$	30/256	8.86×10^{-4}	1.7470×10^{-2}	
	30/512	3.68×10^{-4}	7.0551×10^{-3}	2.4763
	30/1024	1.68×10^{-4}	3.2623×10^{-3}	2.1626
$t = 10.0$	30/256	2.64×10^{-4}	1.1558×10^{-2}	
	30/512	1.10×10^{-4}	5.1806×10^{-3}	2.2310
	30/1024	5.02×10^{-5}	2.5615×10^{-3}	2.0225

Table 6
Errors for peakon–antipeakon interaction in the nonsymmetric case.

	$t = 2$	$t = 3$	$t = 4$	$t = 5$	$t = 6$
E_1	-5.85×10^{-5}	5.87×10^{-5}	7.53×10^{-4}	4.35×10^{-5}	3.25×10^{-4}
L_∞	3.66×10^{-2}	4.95×10^{-2}	4.84×10^{-2}	3.81×10^{-2}	2.89×10^{-2}

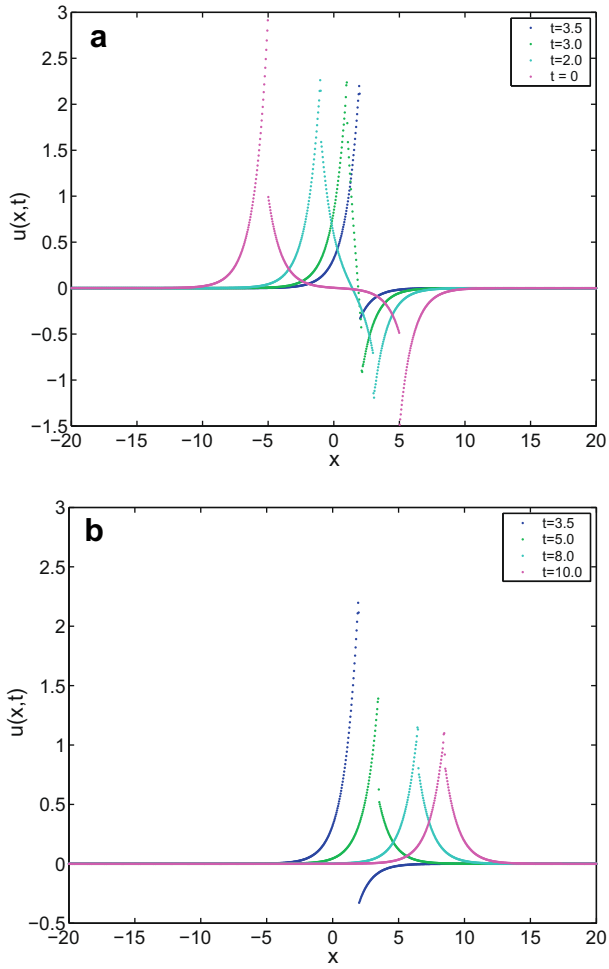

Fig. 6. The snapshots for the interaction between two shockpeakon solutions: (a) before the collision; (b) after the collision.

The simulations are carried out in a domain $[-10,10]$ with 2^M equispaced grid points up to $t = 8.0$. In Fig. 7, we show a 3D plot of the numerical solution by using 2^8 grid points. Since an (almost) exact solution is available [36], we computed the relative L_1 error, defined by

$$L_1 = \max \frac{\sum_j |u_j^n - \tilde{u}_j^n|}{\sum_j |u_j^n|}, \tag{25}$$

where u_j^n and $\tilde{u}_j^n$ denote the exact solution and the numerical solution at $j\Delta x,\ n\Delta t$, respectively. The results are reported in Table 7.

3.3. General initial value problems

We compute the time evolutions of the DP equation starting from several non-exact initial conditions. The value of κ is assumed to be zero except the last example.

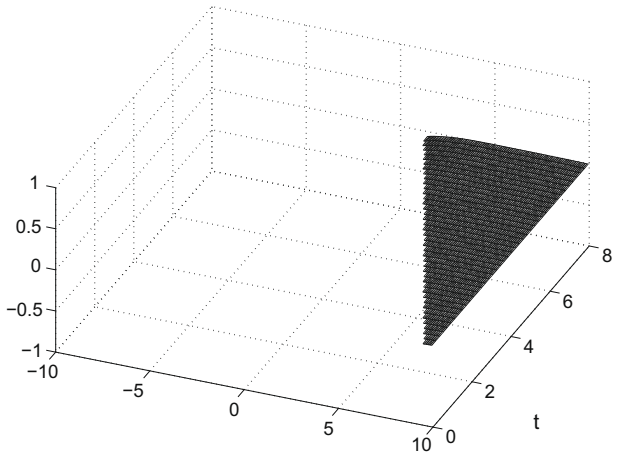

3.3.1. Wave breaking

Liu and Yin [33] showed that wave-breaking can occur in the DP equation. Briefly speaking, assume $u_0 \in H^s(\mathbb{R}), s > \frac{3}{2}$, and there exists $x_0 \in \mathbb{R}$ such that the momentum density $m_0(x) = u_0(x) - u_{0,xx}(x)$ changes the sign from positive to negative at $x = x_0$, then the corresponding solution breaks in finite time $T < +\infty$, i.e. the wave profile remains bounded but its slope becomes infinity in finite time T. The shock waves usually appear afterwards.

Example 3.7. We verify the above theoretical results by an example, whose initial condition is given by

$$u_0(x) = \operatorname{sech}^2(d(x - x_0)), \tag{26}$$

where d is a parameter to control the width of the initial profile. Figs. 8 and 9 show the results for $d = 0.3, d = 2.0$, respectively. When $d = 0.3$, several peakons are developed from the initial condition. However, for $d = 2.0$, a shockpeakon and an antipeakon are developed.

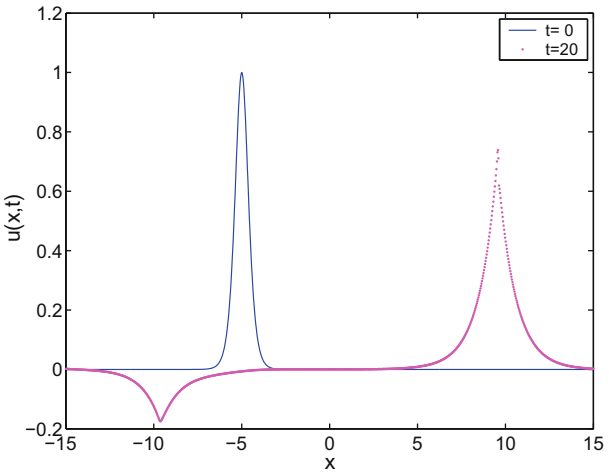

Fig. 9. The numerical solution from initial condition (26) with $d = 2.0$.

The results of wave breaking phenomena for the DP equation [33] give an explanation of the above intriguing fact. One can easily calculate

$$u_0(x) - u_{0,xx}(x) = \operatorname{sech}^2[d(x - x_0]((1 - 4d^2) + 6d^2\operatorname{sech}^2[d(x - x_0]), \tag{27}$$

which remains positive if $d < 1/2$, and changes the sign if $d > 1/2$ for certain values of x. Accordingly, wave breaking does not occur when $d = 0.3$, but it occurs, and a shockpeakon is developed for $d = 2.0$.

Example 3.8. An example whose initial condition given by

$$u_0(x) = e^{0.5x^2}\sin(\pi x), \quad x \in [-2, 2] \tag{28}$$

is computed. Fig. 10(a) and (b) shows the computed solution up to $t = 1.3$, which agrees with the numerical results in [9]. It is checked here that $m_0(x) = u_0(x) - u_{0,xx}(x)$ changes the sign from positive from negative at $x \approx \pm 1.22$. Therefore, we remark that the breaking of the initial continuous wave, leading to the formation of two shock waves, can be theoretically explained by the result in [33].

3.3.2. Other general initial value problems

To compare with existing numerical methods of the DP equation, we further compute several examples.

Example 3.9. We consider a discontinuous initial condition

$$u_0(x) = 2e^x\chi_{(-\infty,0)}(x) + 2\chi_{(0,1)}(x). \tag{29}$$

The evolution is numerically solved in a domain $[-5, 15]$ with 2^M equispaced grid points. Fig. 11 shows the numerical solutions at $t = 2.0, 5.0$, together with the initial profile. The L_1 errors and the rate of convergence are illustrated in Table 8. Since the exact solution is unknown, the numerical solution with 2^{10} grid points is used as a reference solution.

Example 3.10. An algebraically-decayed initial condition given by

$$u_0(x) = \frac{2}{1 + x^2} \tag{30}$$

is computed on a domain $[-30, 30]$ with $N = 2^M$ grid points. Similar to Example 3.9, the L_1 errors are calculated by using the numerical solution of $N = 1024$ as the reference solution. The results are showed in Table 9. Fig. 12 shows the numerical solution at $t = 2.0, 5.0$.

Example 3.11. In the last example, we show the evolution of the initial condition (26) is very different for $\kappa \neq 0$. The parameters in the initial condition are $d = 0.1, x_0 = -50$, and the computation domain is $[-100, 100]$. The value of κ is chosen as 0.01, which implies a very small dispersion term, corresponding to the dispersiveness DP equation. The initial profile and the approximate solution at $t = 60$ are shown in Fig. 13. This result is similar to the result of the dispersiveness CH equation [23], i.e. a peakon train is generated.

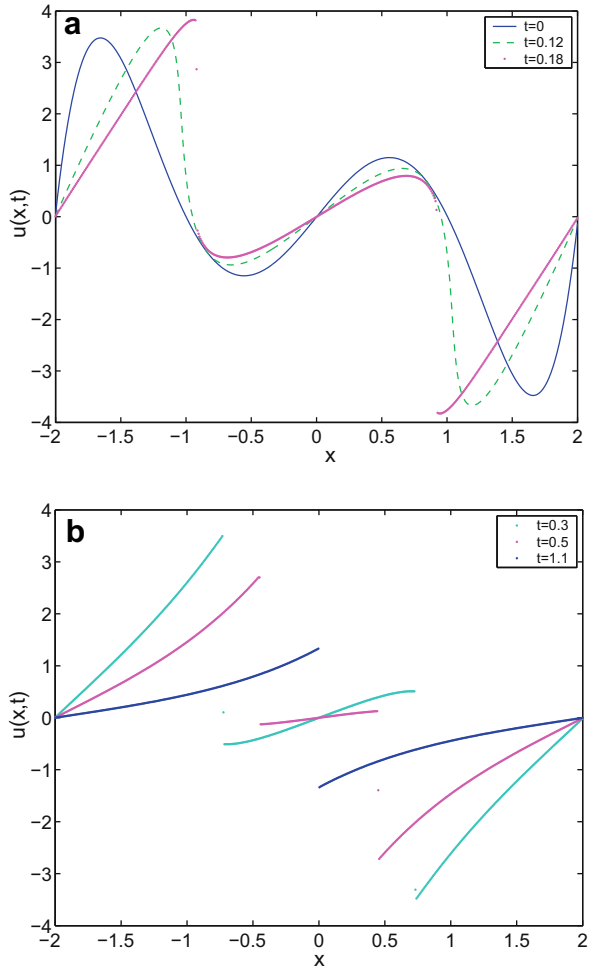

Fig. 10. The snapshots for the time evolution of the initial condition (28).

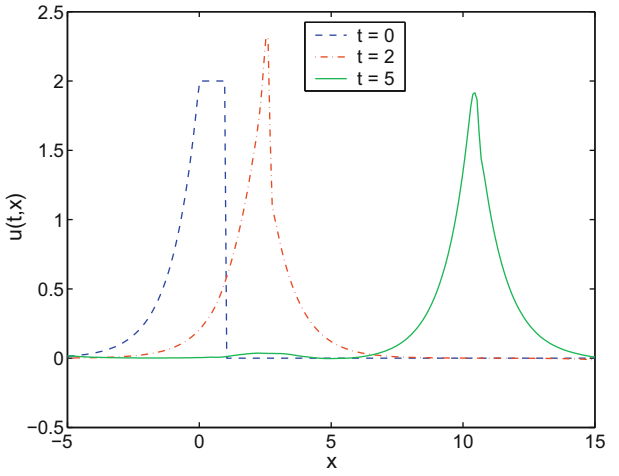

Fig. 11. The numerical solution from initial condition (29).

Table 8
Errors for numerical solution of (29).

Time	Δx	L_1	Rate of convergence
$t = 2.0$	20/64	3.88×10^{-1}	
	20/128	1.14×10^{-1}	3.4035
	20/256	4.05×10^{-2}	2.8148
$t = 5.0$	20/64	7.67×10^{-1}	
	20/128	1.44×10^{-1}	5.3264
	20/256	4.86×10^{-2}	2.9629

Table 9
Errors for numerical solution of (30).

Time	Δx	L_1	Rate of convergence
$t = 2.0$	20/64	4.06×10^{-1}	
	20/128	2.12×10^{-1}	1.9151
	20/256	1.60×10^{-1}	1.3250
$t = 5.0$	20/64	1.11×10^{0}	
	20/128	6.33×10^{-1}	1.7536
	20/256	3.28×10^{-1}	1.9299

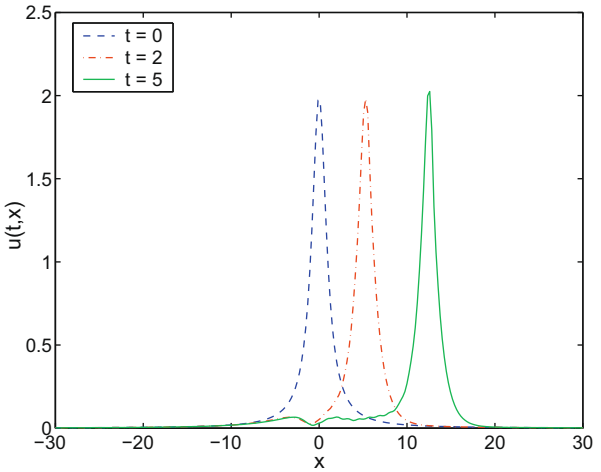

Fig. 12. The numerical solution from initial condition (30).

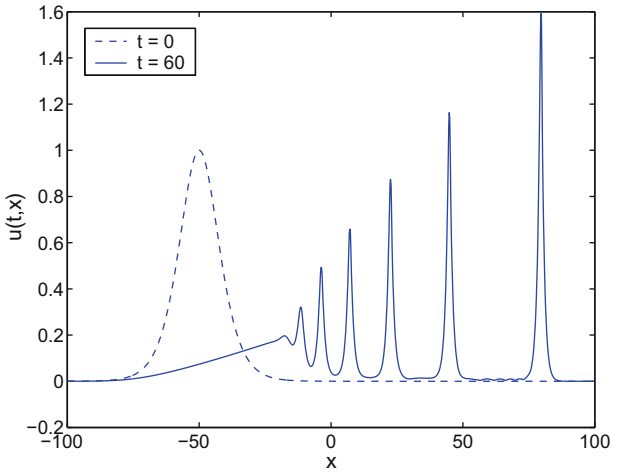

Fig. 13. The numerical solution from initial condition (26) with $d = 0.1$ and $\kappa = 0.01$.

4. Concluding remarks and comments

We proposed an operator splitting method for the DP equation, by which the DP equation is decomposed into the Burgers equation and the BBM equation. We apply a second order TVD scheme to the Burgers equation, and a linearized implicit finite difference method of the second order for the BBM equation. Then, the Strang splitting method is used to construct the solution in one time step. Therefore, the proposed operator splitting method is a second order method for the smooth solution. The method also deals with the discontinuous solutions such as peakon and shockpeakon and the wave breaking phenomena with good accuracy.

We carried out extensive numerical computations with various initial conditions, and summarized the results as follows:

1. The method is of second order and is confirmed by a single smooth soliton solution.
2. The numerical solutions of one peakon propagation and two-peakon interaction are in good agreement with exact solutions.
3. The operator splitting method captures the formation and propagation of shockpeakon with good accuracy.
4. The operator splitting method catches the wave breaking phenomena well, and verified the theoretical prediction.

In conclusion, the proposed splitting method is an effective method to deal with both smooth and discontinuous solutions of the DP equation. It is expected to be used as a tool to study the rich wave phenomena of the DP equation, along with some theoretical methods.

Acknowledgements

The authors are very grateful to Professor P. Lax for his encouragements and comments on the present work. The authors are grateful for the comments by anonymous reviewers which lead to the improvement of the present paper. The work of Feng was supported partly by the US Army Research Office under Contract No. W911NF-05-1-0029. The work of Liu was partially supported by the NSF Grant DMS-0906099.

References

[1] R. Artebrant, H.J. Schroll, Numerical simulation of Camassa–Holm peakons by adaptive upwinding, Appl. Numer. Math. 56 (2006) 695.
[2] R. Beals, D.H. Sattinger, J. Szmigielski, Multipeakons and the classical moment problem, Adv. Math. 154 (2000) 229.
[3] T.B. Benjamin, J.L. Bona, J. Mahony, Model equations for long waves in nonlinear dispersive systems, Phil. R. Soc. London, Ser. A 272 (1972) 47.
[4] R. Camassa, D.D. Holm, An integrable shallow water equation with peaked solitons, Phys. Rev. Lett. 71 (1993) 1661.
[5] R. Camassa, D.D. Holm, J. Hyman, A new integrable shallow water equation, Adv. Appl. Mech. 31 (1993) 1.
[6] R. Camassa, Characteristics and the initial value problem of a completely integrable shallow water equation, DCDS-B 3 (2003) 115.
[7] R. Camassa, J. Huang, L. Lee, On a completely integrable numerical scheme for a nonlinear shallow-water wave equation, J. Nonlinear Math. Phys. 12 (2005) 146.
[8] R. Camassa, J. Huang, L. Lee, Integral and integrable algorithms for a nonlinear shallow-water wave equation, J. Comp. Phys. 216 (2006) 547.
[9] G.M. Coclite, K.H. Karlsen, N.H. Risebro, Numerical schemes for computing discontinuous solutions of the Degasperis–Procesi equation, IMA J. Numer. Anal. 28 (2008) 80.
[10] G.M. Coclite, K.H. Karlsen, N.H. Risebro, A convergent finite difference scheme for the Camassa–Holm equation with general H^1 initial data, SIAM J. Numer. Anal. 46 (2008) 1554.
[11] G.M. Coclite, K.H. Karlsen, On the well-posedness of the Degasperis–Procesi equation, J. Funct. Anal. 233 (2006) 60.
[12] G.M. Coclite, K.H. Karlsen, On the uniqueness of discontinuous solutions to the Degasperis–Procesi equation, J. Differential Eq. 234 (2007) 142.
[13] G.M. Coclite, K.H. Karlsen, Bounded solutions for the Degasperis–Procesi equation, Boll. Unione Mat. Ital. Sez. B Artic. Ric. Mat. 1 (2008) 439.
[14] D. Cohen, B. Owren, X. Raynaud, Multi-symplectic integration of the Camassa–Holm equation, J. Comp. Phys. 227 (2008) 5492.
[15] A. Constantin, On the scattering problem for the Camassa–Holm equation, R. Soc. Lond. Proc. Ser. A. Math. Phys. 457 (2001) 659.
[16] A. Constantin, D. Lannes, The hydrodynamical relevance of the Camassa–Holm and Degasperis–Procesi equations, Arch. Rantional Mech. Anal. 192 (2009) 165.
[17] A. Constantin, W.A. Strauss, Stability of peakons, Comm. Pure Appl. Math. 53 (2000) 603.
[18] A. Degasperis, D.D. Holm, A.N.W. Hone, A new integral equation with peakon solutions, Theor. Math. Phys. 133 (2002) 1463.
[19] A. Degasperis, M. Procesi, Asymptotic integrability, in: A. Degasperis, G. Gaeta (Eds.), Symmetry and Perturbation Theory, World Scientific Publishing, 1999, pp. 23–37.
[20] J. Escher, Y. Liu, Z. Yin, Global weak solutions and blow-up structure for the Degasperis–Procesi equation, J. Funct. Anal. 241 (2006) 457.
[21] J. Escher, Y. Liu, Z. Yin, Shock waves and blow-up phenomena for the periodic Degasperis–Procesi equation, Indiana Univ. Math. J. 56 (2007) 87.
[22] B.F. Feng, T. Mitsui, A finite difference method for the Korteweg-de Vries and the Kadomtsev-Petviashvili equations, J. Comp. Appl. Math. 90 (1998) 95.
[23] B.F. Feng, K. Maruno, Y. Ohta, A self-adaptive mesh method for the Camassa–Holm equation, preprint.
[24] A. Fokas, B. Fuchssteiner, Symplectic structures their Bäcklund transformation and hereditary symmetries, Physica D 4 (1981) 47.
[25] A. Harten, High resolution schemes for hyperbolic conservation laws, J. Comput. Phys. 49 (1983) 357–393.
[26] H.A. Hoel, A numerical scheme using multi-shock peakons to compute solutions of the Degasperis–Procesi equation, Elect. J. Diff. Eq. 2007 (2007) 1.
[27] H. Holden, X. Raynaud, Convergence of a finite difference scheme for the Camassa–Holm equation, SIAM J. Num. Anal. 44 (2006) 1655.
[28] H. Holden, X. Raynaud, A convergent numerical scheme for the Camassa–Holm equation based on multipeakons, Discrete Contin. Dyn. Syst. 14 (2006) 50.
[29] H. Kalisch, J. Lenells, Numerical study of traveling-wave solutions for the Camassa–Holm equation, Chaos, Solitons & Fractals 25 (2005) 287.
[30] R.J. Leveque, Finite Volume Methods for Hyperbolic Problems, Cambridge University Press, New York, 2002.
[31] R.S. Johnson, Camassa–Holm, Korteweg-de Vries and related models for water, J. Fluid Mech. 455 (2002) 63.
[32] Z. Lin, Y. Liu, Stabiltiy of peakons for the Degasperis–Procesi equation, Comm. Pure Appl. Math. LXII (2008) 1.
[33] Y. Liu, Z. Yin, Global existence and blow-up phenomena for the Degasperis–Procesi equation, Comm. Math. Phys. 267 (2006) 801.
[34] H. Lundmark, J. Szmigielski, Multi-peakon solutions of the Degasperis–Procesi equation, Inv. Prob. 19 (2003) 1241.
[35] H. Lundmark, J. Szmigielski, Degasperis–Procesi peakons and the discrete cubic string, Int. Math. Res. Pap. 2005 (2003) 53.

[36] H. Lundmark, Formation and dynamics of shock waves in the Degasperis–Procesi equation, J. Nonlinear Sci. 17 (2007) 169.
[37] Y. Matsuno, Multisoliton solutions of the Degasperis–Procesi equation and their peakon limit, Inv. Prob. 21 (2005) 1553.
[38] Y. Matsuno, Multisoliton solutions of the Degasperis–Procesi equation, Inv. Prob. 21 (2005) 2085.
[39] T. Matsuo, H. Yamaguchi, An energy-conserving Galerkin scheme for a class of nonlinear dispersive equations, J. Comput. Phys. 228 (2009) 4346.
[40] Y. Ohta, K. Maruno, B.F. Feng, An integrable semi-discretization of the Camassa–Holm equation and its determinant solution, J. Phys. A: Math. Theor. 41 (2008) 355205.
[41] A. Parker, On the Camassa–Holm equation and a direct method of solution I. Bilinear form and solitary waves, R. Soc. Lond. Proc. Ser. A 460 (2004) 2929.
[42] G. Strang, on the construction and comparison of difference schemes, SIAM J. Numer. Anal. 5 (1968) 506.
[43] Y. Xu, C.-W. Shu, A local discontinuous Galerkin method for the Camassa–Holm equation, SIAM J. Numer. Anal. 46 (2008) 1998.